Time Shift Governor for Constraint Satisfaction during Low-Thrust Spacecraft Rendezvous in Near Rectilinear Halo Orbits

Taehyeun Kim, Kaiwen Liu, Ilya Kolmanovsky, and Anouck Girard

Abstract-A parameter governor-based control scheme is developed to enforce various constraints, such as the Line of Sight (LoS) cone angle, the thrust limit, and the relative approach velocity during rendezvous missions in a near rectilinear halo orbit (NRHO) in the Earth-Moon system. The parameter governor is an add-on scheme to the nominal closed-loop system, which dynamically adjusts controller parameters in order to enforce the constraints. For the application to the rendezvous mission, we utilize the Time Shift Governor (TSG) which time shifts the target trajectory commanded to the Deputy spacecraft controller. The time shift is gradually reduced to zero so that the virtual target trajectory gradually converges to the Chief spacecraft trajectory as time evolves, and the rendezvous mission can be accomplished. Simulation results are reported that demonstrate the effectiveness of the proposed control scheme.

I. INTRODUCTION

Spacecraft rendezvous technology is vital to present and future space missions. The rendezvous missions make it possible to assemble, maintain, and repair satellites and space stations. For example, the Lunar Gateway mission involves multiple rendezvous maneuvers to assemble a space station that will enable human deep space exploration in cislunar space [1].

The growing complexity of rendezvous mission requirements also motivates a transition from humanguided operations to autonomous rendezvous. For instance, the ISS has been serviced by the SpaceX Cargo Dragon spacecraft, Progress spacecraft, and Cygnus spacecraft. More autonomous spacecraft rendezvous missions are planned including the National Aeronautics and Space Administration's On-Orbit servicing, Assembly, and Manufacturing 1 (OSAM-1) mission [2] and the European Space Agency's ClearSpace-1 mission [3].

As the complexity of rendezvous missions increases, many system constraints and limits, such as Line-of-Sight (LoS) cone angle constraints and thrust limits, need to be strictly enforced, because violation of these constraints can lead to failure of the entire mission. The goal of this paper is to propose an approach for enforcing constraints in spacecraft rendezvous missions on halo orbits based on the Time Shift Governor (TSG).

Taehyeun Kim, Kaiwen Liu, Ilya Kolmanovsky, and Anouck Girard are with the Department of Aerospace Engineering, University of Michigan, Ann Arbor, 48109 MI, USA. {taehyeun, kwliu, ilya, anouck}@umich.edu. This research is supported, in part, by Air Force Office of Scientific Research Grant number FA9550-20-1-0385 and National Science Foundation Award CMMI-1904394.

In the restricted three-body problem (R3BP) setting [4], [5], a halo orbit is a periodic, three-dimensional orbit, where a third body's motion is determined by the gravitational pull of the two celestial bodies (called primaries) assuming the third body has negligible mass. Such halo orbits have received increasing attention for actual missions because of their advantages, such as remaining in a fixed position relative to a target body, having an unobstructed view, and reducing fuel consumption [6]. A spacecraft called the International Sun-Earth Explorer-3 first entered a halo orbit near the L_1 Lagrange point of the Sun-Earth system in November 1978 [7]. In 1996, the Solar and Heliospheric Observatory (SOHO) also used the interior Sun-Earth L_1 point for a joint ESA/NASA mission to study the Sun. Moreover, the James Webb Space Telescope was placed into a halo orbit near the Sun-Earth L_2 point in 2022.

In this paper, a near rectilinear halo orbit (NRHO), which is a subclass of halo orbits near the L_2 Lagrange point in the Earth-Moon system, is considered as a desired reference trajectory. Particular NRHOs have the advantages of the existence of low-energy transfer orbits [8], good stability properties, clear views of the Earth, and favorable resonance characteristics that enable them to avoid eclipses [9]. There is a growing interest in NRHOs in the space community, as evidenced by the NASA Artemis [10] and CAPSTONE [11], [12] missions.

The dynamics of relative motion have been previously studied to address spacecraft rendezvous in proximity to halo orbits. Scheeres and Vinh [13] have studied the relative motion of two spacecraft and stabilization of the secondary spacecraft to the primary spacecraft in an unstable halo orbit; their analysis relied on linearized dynamics and accounted for long-term and short-term motions [13]. Bucchioni and Innocenti [14] describe a dynamic model for the translational relative motion and attitude relative motion in the elliptic restricted three-body problem (ER3BP) and circular restricted three-body problem (CR3BP). Colagrossi and Lavagna [15] present a coupled orbit-attitude dynamical model that accounts for the effects of large structural flexibility.

Several control approaches have been demonstrated for station keeping [16], [17], orbit maneuvering [18], and spacecraft rendezvous [19] in the Earth-Moon NRHOs. A PD controller is implemented for the spacecraft rendezvous in halo orbit near the Earth-Moon L_2 point in

[20]. A chance-constrained MPC approach is proposed to effect the spacecraft rendezvous in the Earth-Moon NRHOs in [19].

In this work, we implement a Time Shift Governor (TSG), an approach that had been previously applied to constrained spacecraft formation control in circular Earth orbits in the setting of a Two Body problem [21], [22]. The TSG adjusts only one parameter, the time shift, and is straightforward to implement. It belongs to a larger class of methods for coordinating motions by adjusting the space versus time assignments along prescribed trajectories, see, e.g., [23] for a different approach along these lines that has been applied to multirotor unmanned aerial vehicles.

TSG is a variant of the parameter governor [24], i.e., it is an add-on scheme that alters parameters in the nominal control system to satisfy pointwise-in-time state and control constraints. Compared to more general nonlinear model predictive controllers, parameter governors provide a solution with lower computational effort because they rely on solving online only a low-dimensional optimization problem with a few parameters that can take discrete values. In this paper, we apply the TSG to a spacecraft rendezvous in a halo orbit in the Circular R3BP (CR3BP) setting.

This paper is organized as follows: In Section II, we summarize the spacecraft translational dynamics model in the CR3BP setting, the nominal controller, as well as the constraints considered during the rendezvous mission. Then, in Section III, we introduce the TSG to enforce the constraints. Simulation results of the rendezvous mission are reported in Section IV, and demonstrate the ability of the TSG to enforce constraints. Finally, conclusions are drawn and future research directions are outlined in Section V.

II. PROBLEM FORMULATION

In this paper, we consider a spacecraft rendezvous mission in a near rectilinear halo orbit (NRHO) subject to various mission-specific constraints. During the rendezvous mission, the secondary (Deputy) spacecraft locates in front of the primary (Chief) spacecraft in the orbital track direction and is further away in the orbital track at the initial point. The reverse situation (the Deputy is behind the Chief) can be addressed similarly. In this paper, we use subscripts c and d to denote the Chief spacecraft and the Deputy spacecraft, respectively, and we use subscript i to denote spacecraft that can either be the Chief or the Deputy.

A. Coordinate systems

In this work, the barycentric frame and a local frame (LVLH) are employed. The spacecraft dynamics are first expressed in the barycentric frame. This barycentric frame is defined by $b : \{O_b, i_b, j_b, k_b\}$ where O_b is the barycenter of the Earth-Moon system, i_b coincides with the direction from the Earth to Moon, k_b is parallel to

the Earth-Moon system angular momentum vector, and j_b completes a right-handed frame, as shown in Figure 1.

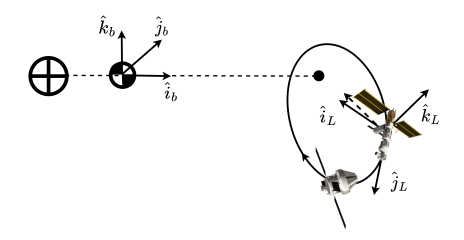


Fig. 1: Barycentric and LVLH frames in the Earth-Moon system.

Additionally, the LVLH frame is also defined as $L: \{O_c, i_L, j_L, k_L\}$ where O_c is located at the Chief spacecraft position, j_L aligns with the velocity vector of the Chief, k_L is the cross product of the normalized Moon position vector relative to the Chief with j_L , and i_L completes the right-handed system.

B. Circular Restricted Three-Body Problem

The spacecraft dynamics are modeled in the setting of the circular restricted three-body problem (CR3BP) [4], [5]. The equations of motion can be written as

$$\dot{X}_i(\tau) = f(\tau, X_i(\tau), u_i(\tau)), \tag{1}$$

where $X_i = [x_i, y_i, z_i, \dot{x}_i, \dot{y}_i, \dot{z}_i]^\mathsf{T}$, $i \in \{c, d\}$ denotes the state of the spacecraft, which consists of position and velocity, $u_i = [u_{x,i}, u_{y,i}, u_{z,i}]^\mathsf{T}$, $i \in \{c, d\}$ denotes the control input to the spacecraft, and $\tau \in \mathbb{R}_{\geqslant 0}$ denotes the non-dimensional time. Note that the spacecraft's state and control input for $i \in \{c, d\}$ are expressed in the barycentric frame.

The governing equations of motion for the CR3BP are given in non-dimensional form as [4], [5]:

$$\ddot{x}_{i} = 2\dot{y}_{i} + x_{i} - \frac{(1-\mu)(x_{i} + \mu)}{r_{1,i}^{3}} - \frac{\mu(-1+x_{i} + \mu)}{r_{2,i}^{3}} + u_{x,i},$$

$$\ddot{y}_{i} = -2\dot{x}_{i} + y_{i} - \frac{y_{i}(1-\mu)}{r_{1,i}^{3}} - \frac{\mu y_{i}}{r_{2,i}^{3}} + u_{y,i},$$

$$\ddot{z}_{i} = -\frac{z_{i}(1-\mu)}{r_{1,i}^{3}} - \frac{\mu z_{i}}{r_{2,i}^{3}} + u_{z,i},$$
(2)

where subscript $i \in \{c, d\}$ denotes either the Chief or the Deputy spacecraft, $r_{1,i}$ and $r_{2,i}$ can be expressed as,

$$r_{1,i} = [(x_i + \mu)^2 + y_i^2 + z_i^2]^{1/2},$$

$$r_{2,i} = [(x_i - 1 + \mu)^2 + y_i^2 + z_i^2]^{1/2},$$
(3)

and $\mu=m_m/(m_e+m_m)$ is the mass ratio of the secondary body to the total system, with m_e being the mass of the Earth and m_m being the mass of the Moon.

Note that the units of states and control inputs can be dimensionalized by applying the distance scale of D, where D is Earth-Moon distance, and the time scale

of 1/n, where n stands for the mean motion of Moon orbiting around the Earth, i.e., $n = \sqrt{G(m_e + m_m)/D^3}$, where G is the universal gravitational constant.

C. Nominal Controller

The objective of the nominal controller is to track a state trajectory in the barycentric frame that corresponds to a commanded orbital position on NRHO (either that of Chief spacecraft or of a virtual target corresponding to Chief spacecraft advanced along the orbital track). We use a linear-quadratic regulator (LQR) with a constant gain as our nominal controller, while noting that TSG is applicable to other nominal controller choices, including LQR with the gain re-computed along the orbit, as long as the nominal controller is (locally) stabilizing.

The Chief spacecraft is assumed to operate in NRHO with unforced natural motion (i.e., $u_c(\tau)=0, \forall \tau \in \mathbb{R}_{\geqslant 0}$), while the Deputy is controlled by the feedback law

$$u_d(\tau) = K(X_d(\tau) - X_v(\tau)), \tag{4}$$

where $X_v(\tau)$ is the virtual target for the Deputy spacecraft, and K is the frozen-in-time LQR gain which is computed for the linearization of (1) at a selected point on the orbit. The linearization of (1) has the following form:

$$\delta \dot{X} = \left[\frac{\partial f}{\partial X} (X_v(\tau), 0) \right] \delta X + \left[\frac{\partial f}{\partial u_d} (X_v(\tau), 0) \right] \delta u,$$

$$= A \delta X + B \delta u,$$
(5)

where

$$\delta X(\tau) = X_d(\tau) - X_v(\tau), \quad \delta u(\tau) = u_d(\tau) - 0.$$
 (6)

The nominal LQR controller is designed such that the feedback law defined by (4), when applied to (1), results in (local) closed-loop uniform asymptotic stability of the unforced trajectory $X_v(\tau)$, and, in particular, $X_d(\tau) \to X_v(\tau)$ as $\tau \to \infty$.

D. Constraints

The operation of the Deputy spacecraft is subject to various constraints. In this work, we mainly consider three types of constraints to demonstrate the effectiveness of the proposed approach. These include LoS cone angle constraint, thrust limits, and an approach velocity constraint in the vicinity of the Chief spacecraft.

The objective of the rendezvous mission is to bring the Deputy spacecraft to close proximity of the Chief spacecraft and proceed to docking. During the approach, the Deputy spacecraft has to remain within a prescribed Line of Sight (LoS) cone. The LoS cone angle constraint is defined with LoS half-cone angle α as

$$h_1 = -v(X_c)^T p(X_d - X_c) + \cos(\alpha) ||v(X_c)|| ||p(X_d - X_c)|| \le 0,$$
(7)

where v(X) designates the velocity vector and p(X) designates the position vector corresponding to the full state X.

The thrust that the Deputy spacecraft can develop is limited, leading to a constraint,

$$h_2 = ||u_d|| - u_{\text{max}} \le 0, \tag{8}$$

where $u_{\rm max}$ is the maximum magnitude of the control input. Rather than handling (8) as a constraint by TSG, an alternative approach, which can lead to faster response [25], is to enforce (8) using saturation. Such a saturation preserves the direction of the control input and limits its magnitude to the maximum value $u_{\rm max}$:

$$u_{d}(\tau) := \begin{cases} u_{d}(\tau), & \text{if } ||u_{d}(\tau)|| \leq u_{\text{max}}, \\ u_{\text{max}} \frac{u_{d}(\tau)}{||u_{d}(\tau)||}, & \text{if } ||u_{d}(\tau)|| > u_{\text{max}}. \end{cases}$$
(9)

With (9) used to enforce (8), the TSG must also account for the control input being saturated in its prediction model.

When the Deputy spacecraft is in the vicinity of the Chief spacecraft, a constraint on the relative velocity between the Deputy spacecraft and the Chief spacecraft is imposed to avoid potential high speed collisions between them. As a result, the constraint on the magnitude of the relative velocity is only active when the Deputy spacecraft is near the Chief spacecraft, i.e.,

$$||p(X_d - X_c)|| \leqslant \gamma_1, \tag{10}$$

in which case, the relative velocity is bounded by a linearly decreasing function of the relative distance to the Chief location,

$$h_3 = ||v(X_d - X_c)|| - \gamma_2 ||p(X_d - X_c)|| - \gamma_3 \le 0, (11)$$

where γ_2 and γ_3 are constant parameters.

Additional constraints could be included such as constraining the final state of the Deputy spacecraft along the predicted trajectory to a small terminal region around the virtual target to ensure stability. Such a constraint has not been added in this paper as the nominal closed-loop system remained stable for the maneuvers considered.

III. TIME SHIFT GOVERNOR

In this paper, we adopt the TSG to enforce the constraints in our halo orbit rendezvous problem. The proposed control scheme is shown in Figure 2, where the TSG augments a nominal closed-loop system consisting of spacecraft dynamics and the nominal LQR controller. If it were not for constraints (and assuming closed-loop stability), to perform the rendezvous with the Chief spacecraft, the state trajectory of the Chief spacecraft along NRHO could be simply commanded to the nominal controller of the Deputy spacecraft.

To avoid violation of the constraints, the TSG commands to the nominal controller of the Deputy spacecraft a time shifted trajectory of the Chief spacecraft, i.e., the commanded state for the Deputy spacecraft at time τ is given by

$$X_v(\tau) = X_c(\tau + \tau_{\text{lead}}), \tag{12}$$

where τ_{lead} is the time shift. Assuming the Deputy spacecraft is further along the orbital track as compared

to the Chief spacecraft, we restrict the time shift to non-negative values, i.e., $\tau_{\text{lead}} \geqslant 0$, and set an upper bound of τ_{lead} as an initial admissible time shift which results in constraint satisfaction (assumed to exist by prepositioning Deputy spacecraft if necessary). The TSG then minimizes the time shift, $\tau_{\text{lead}} \geqslant 0$, at discrete-time instants subject to the condition that the predicted closed-loop trajectory of the Deputy spacecraft and the predicted open loop trajectory of Chief spacecraft over a sufficiently long prediction horizon satisfy the imposed state and control constraints. Figure 3 shows an illustration of the Chief, the Deputy and the virtual target (time shifted Chief spacecraft state commanded to the nominal controller) during operations.

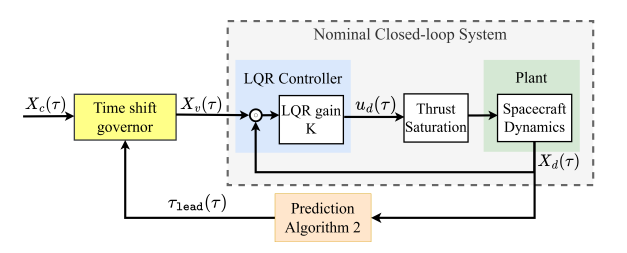


Fig. 2: Diagram of the nominal closed-loop system augmented with the TSG to enforce constraints.

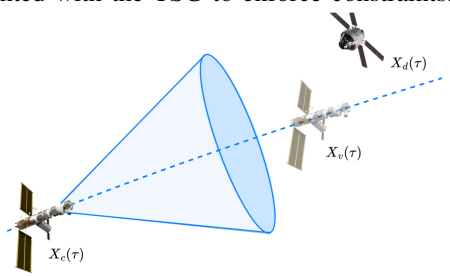


Fig. 3: The Chief, the Deputy, and the virtual target spacecraft in the orbital track.

Following the developments in [22], [21], [24], it can be shown that if a feasible τ_{lead} exists at the initial time instant, the prediction horizon is sufficiently long, the nominal controller is stabilizing and constraints strictly hold in *steady-state* corresponding to any constant virtual target, then constraints are guaranteed to be satisfied for all future times. As the Deputy spacecraft is controlled by the nominal controller to the target $X_v(\tau)$ and τ_{lead} is reduced by the TSG, the Deputy spacecraft is made to safely approach the Chief spacecraft. Formal finite-time convergence guarantees of τ_{lead} to zero and $X_v(\tau)$ to $X_c(\tau)$ can be given under the assumption of strict steady-state feasibility and rejection of sufficiently small changes in τ_{lead} by the TSG [24], [26].

The process of finding τ_{1ead} using bisections is summarized in Algorithms 1 and 2. In Algorithm 1, we first set the initial time shift parameter $\tau_{1ead,0} \in \mathbb{R}_{>0}$, such that (4), (12) with $\tau_{1ead} = \tau_{1ead,0}$ results in trajectories that do not violate constraints. In (12), we limit the time shift parameter τ_{1ead} to

$$\tau_{\text{lead}}(\tau) \in \mathcal{T} = \{ \tau \in \mathbb{R}_{\geq 0} : 0 \leqslant \tau \leqslant \tau_{\text{lead},0} \}, \quad (13)$$

where \mathcal{T} denotes the time shift parameter set.

In Lines 4-8, the algorithm finds the minimal admissible time shift parameter iteratively, where ψ is the minimum adjustment to the τ_{lead} during each update and P_{ref} is the prediction horizon. The feasibility of the time shift parameter is evaluated by the prediction (Algorithm 2), which checks whether the virtual target determined by the time shift parameter can satisfy all imposed constraints for all time instants over the prediction horizon, i.e., $\forall \tau \in [\tau, \tau + P_{\text{ref}}]$. In Line 6 of Algorithm 2, the prediction is performed based on forward propagation of the nonlinear model (1), (4) and (9).

Algorithm 1 Time shift governor algorithm

- 1: Select the initial shift parameter $\tau_{\text{lead}} = \tau_{\text{lead},0} \in \mathbb{R}_{\geq 0}$ at $\tau = 0$ s.t. the resulting trajectory satisfies constraints using the selected $\tau_{\text{lead},0}$ in (4) and (12);
- 2: while $au < au_{ ext{end}}$ do
- 3: $\overline{\tau}_{\text{lead}} = \tau_{\text{lead}}, \ \underline{\tau}_{\text{lead}} = 0;$
- 4: while $||\overline{\tau}_{\mathtt{lead}} \underline{\tau}_{\mathtt{lead}}|| > \psi$ do
- 5: Propose a shift parameter:

$$\tau_{\mathtt{lead},\mathtt{m}} = (\overline{\tau}_{\mathtt{lead}} + \underline{\tau}_{\mathtt{lead}})/2;$$

6: Predict the trajectory using the proposed time shift parameter over the time interval $\tau_{\tt pred} = [\tau, \tau + P_{\tt ref}],$

$$\mathbb{1}_{\text{safe}} = \operatorname{Prediction}(X_c(\tau), X_d(\tau), \tau_{\mathtt{lead}, \mathtt{m}}, \tau_{\mathtt{pred}});$$

7: Update the feasible shift parameter bounds,

$$\begin{cases} \overline{\tau}_{\texttt{lead}} = \tau_{\texttt{lead},m}, & \text{if } \mathbb{1}_{\texttt{safe}} = 1, \\ \underline{\tau}_{\texttt{lead}} = \tau_{\texttt{lead},m}, & \text{otherwise;} \end{cases}$$

- 8: end while
- 9: Set $\tau_{\text{lead}} = \overline{\tau}_{\text{lead}}$ and $X_v(\tau) = X_c(\tau + \tau_{\text{lead}});$
- 10: Forward simulate the system over $[\tau, \tau + P_{lead}]$ using (1) and (4);
- 11: $\tau = \tau + P_{\text{lead}}.$
- 12: end while

By construction, the previously computed time shift parameter $\tau_{\text{lead}}(\tau-P_{\text{lead}})$, where P_{lead} is the TSG update period, is feasible at the time instant τ at which TSG updates τ_{lead} ; hence $\tau_{\text{lead}}(\tau-P_{\text{lead}})$ is used as an upper bound on $\tau_{\text{lead}}(\tau)$.

Algorithm 2 Prediction $(X_c(\tau), X_d(\tau), \tau_{\text{lead,m}}, \tau_{\text{pred}})$

- 1: $\mathbb{1}_{safe} = 1$;
- 2: for $\tau \in \tau_{pred}$ do
- 3: Compute control input $u_d(\tau)$ using (4) and (9);
- 4: Compute LoS cone angle constraint h_1
- 5: Compute relative velocity constraint h_3 using (11) if $||p(X_d X_c)|| < 10$ km;
- 6: If $\max(h_1, h_3) \ge 0$, then $\mathbb{1}_{\text{safe}} = 0$ and **break**;
- 7: end for
- 8: return $\mathbb{1}_{safe}$.

After determining the minimal admissible shift parameter, the TSG updates τ_{lead} to this value (Line 9), and the Deputy spacecraft tracks the virtual target determined by

the current $au_{\rm lead}$ (Line 10). The TSG updates $au_{\rm lead}$ again after $P_{\rm lead}$.

IV. SIMULATION RESULTS

In this section, simulation results are reported to demonstrate the ability of the TSG to enforce constraints during the rendezvous mission.

A. Simulation specifications

A near rectilinear halo orbit (NRHO) is considered as a reference trajectory of the Chief spacecraft. Figure 4 shows this reference trajectory for one period $(P_{\rm ref} \sim 6.6 \ {\rm days})$, which corresponds to the initial state $X_c(0) = [1.0220, 0, -0.1821, 0, -0.1031, 0]^{\rm T} [{\rm ND}]$. The prediction horizon for TSG at the time instant τ is selected as $[\tau, \tau + P_{\rm ref}]$.

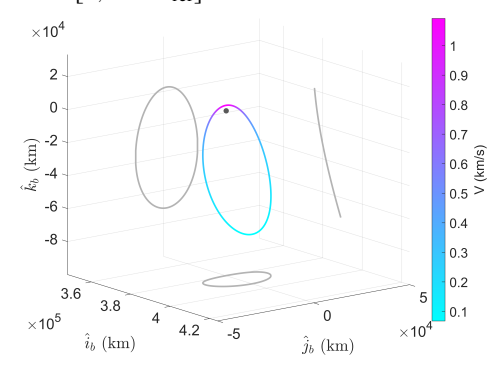


Fig. 4: Reference NRHO trajectory with velocity (color figure), its projection (gray), and Moon (dark gray) in Earth-Moon CR3BP.

In the simulations, we assume that the gravitational constant of the primaries is $G=6.6743\times 10^{-20}~{\rm km}^3\cdot {\rm kg}^{-1}\cdot {\rm s}^{-2}$, the mass of the Earth is $m_e=5.972\times 10^{24}~{\rm kg}$, the mass of the Moon is $m_m=7.3477\times 10^{22}~{\rm kg}$, and the Earth-Moon distance is $D=384,399~{\rm km}$, so that the mean motion is $n=\sqrt{G(m_E+m_M)/D^3}$. We choose the initial time shift as $\tau_{\rm lead,0}=0.0128~{\rm [TU]}=1.3333~{\rm km}$ and the time between subsequent TSG updates of the time shift as $P_{\rm lead}=9.5951\times 10^{-3}~{\rm [TU]}=1~{\rm km}$.

The Deputy spacecraft is controlled by the nominal controller (4) using an LQR gain K corresponding to the following state and control weighting matrices,

$$Q = diag(10^6, 10^6, 10^6, 10^3, 10^3, 10^3),$$

$$R = diag(10, 10, 10),$$

and the linearized model (5) at the initial virtual target $X_c(\tau_{\rm lead,0})$.

In the simulations, the TSG handles constraints introduced in Section II-D and is configured with the following values: The half-cone angle is $\alpha=20$ deg, the maximum thrust magnitude is $u_{\rm max}=0.03$ [ND] = $8.1921\times 10^{-8}{\rm km\cdot s^{-2}}$, and the approach velocity constraint is formed with $\gamma_1=2.6015\times 10^{-5}$ [ND] = 10 km, $\gamma_2=20$ [ND] = 5.3306×10^{-5} s $^{-1}$, and $\gamma_3=0.001$ [ND] = 1.0245×10^{-3} km · s $^{-1}$, where [ND] stands for the non-dimensional unit employed in this paper.

B. Results

Table I summarizes the initial conditions of the Deputy spacecraft and of the virtual target with respect to the Chief spacecraft in the barycentric frame. At the beginning of this simulation, the Deputy is about 609 km forward in the orbital track from the Chief. Algorithm 1 is initialized with $\tau_{\rm lead,0}$ so that the virtual target corresponds to the Deputy position. TSG, after executing at the initial time, $\tau=0$, sets $\tau_{\rm lead}(0)$ so that $\tau_{\rm lead}(0)/n=0.3716$ hr; this corresponds to the virtual target at about 469 km forward from the Chief.

TABLE I: Initial Deputy state and virtual target state ($\tau_{\rm lead,0}=0.0128$) with respect to the Chief in the barycentric frame.

$X_d(0)-X_c(0)$	$m{i}_b$	$oldsymbol{j}_b$	$oldsymbol{k}_b$
Position [km]	-5.9768	-608.5601	22.8060
Velocity [km/s]	-2.0752×10^{-3}	5.3850×10^{-5}	7.9192×10^{-3}
$X_{v}(0)-X_{c}(0)$	$oldsymbol{i}_{b}$	j_b	k_h
	•0	J 0	••0
Position [km]	-11.3610	-466.4400	43.2349

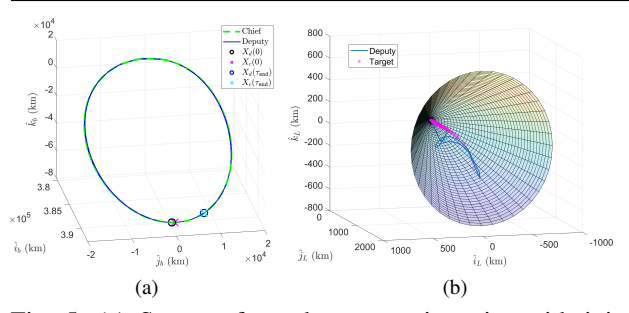


Fig. 5: (a) Spacecraft rendezvous trajectories with initial and final points: $X_c(0)$ (magenta), $X_d(0)$ (black), $X_c(\tau_{end})$ (cyan), $X_d(\tau_{end})$ (blue). (b) The Deputy spacecraft (blue line) and the virtual target (magenta asterisk) trajectories in the LVLH frame, as stated in Section II-A.

Figure 5a shows the three dimensional trajectories of the Chief (green dotted line) and Deputy (solid blue line) with the proposed control scheme during the rendezvous mission. In Figure 5a, the black circle and magenta cross denote the initial Deputy and Chief locations, respectively, while the blue circle and cyan cross indicate the final Deputy and Chief locations. At the end of the simulation, the deviation between the two spacecraft is within 7.6230 m using $\psi=0.01$ in Algorithm 1.

Figure 5b depicts how the TSG governs the spacecraft rendezvous mission by moving the virtual target of the Deputy in the LVLH frame. With the TSG gradually adjusting the virtual target, the proposed control scheme is able to achieve the rendezvous mission while satisfying the imposed constraints.

Figure 6 shows the Deputy spacecraft position relative to the Chief spacecraft and relative to the virtual target in the barycentric frame. The Deputy spacecraft is able to arrive close to the Chief spacecraft and successfully complete the rendezvous mission. Note that there are peaks in both Figures 6a and 6b at around 80 hrs.

These peaks are caused by the sudden increase of the relative velocity as the spacecraft enters the peri-lunar region, which is colored in magenta in Figure 4. Getting into the peri-lunar region instantly boosts the velocity of spacecraft and causes the deviation in the relative position. Since the Deputy spacecraft is closer to the virtual target compared to the Chief spacecraft, this results in a smaller peak in Figure 6b than the one in Figure 6a.

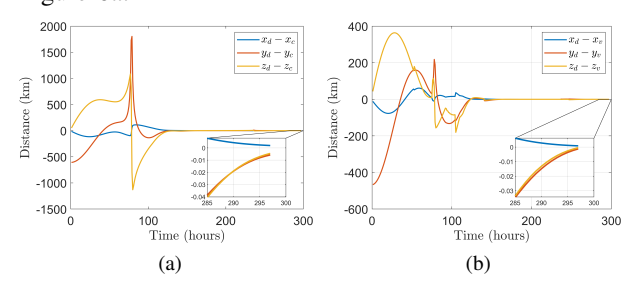


Fig. 6: Time histories of the relative Deputy spacecraft position (a) to the Chief spacecraft and (b) to the virtual target.

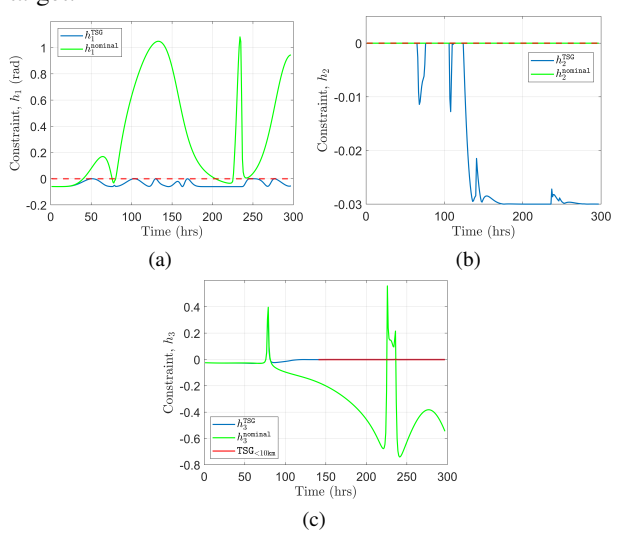


Fig. 7: Time histories of constraints during the rendezvous using the TSG (blue) and only the nominal controller (green): (a) the LoS cone angle constraint h_1 ; (b) thrust constraint h_2 ; (c) the approach velocity constraint h_3 . Note that $h_3 \le 0$ is required only when the Deputy spacecraft is within 10 km distance from the Chief.

In Figures 7a-7c, we compare the performance of using only the nominal controller and our proposed control scheme with the TSG during the rendezvous mission. Figure 7a shows the time history of the LoS cone angle constraint h_1 . The TSG is able to enforce the LoS cone angle constraint, while the nominal controller alone (without TSG) experiences significant constraint violations during the rendezvous mission. Figure 7b shows the thrust constraint h_2 (note that it is handled using saturation as described in (9)). Figure 7c shows the time history of the approach velocity constraint h_3 . The TSG is able to enforce this constraint when it becomes

active (i.e, when the Deputy spacecraft is in the vicinity of the Chief spacecraft). Note that with the nominal controller alone the Deputy spacecraft does not enter a 10 km neighborhood of the Chief spacecraft at all due to thrust saturation, and fails to complete the rendezvous mission.

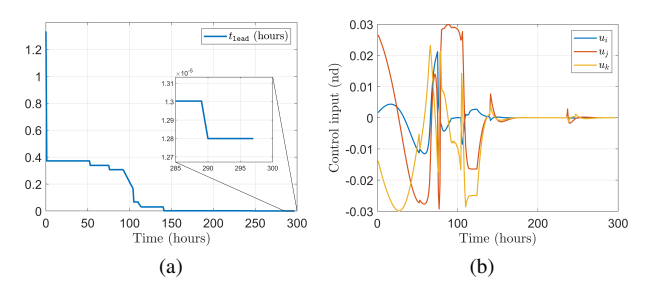


Fig. 8: (a) The evolution of the time shift parameter during the rendezvous in hours $(t_{lead} = \tau_{lead}/n)$. (b) Time history of the Deputy spacecraft control input in the barycentric elements.

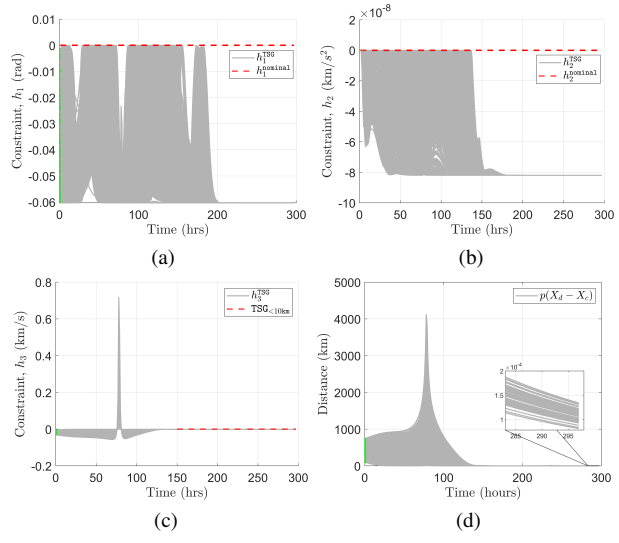


Fig. 9: Time histories of constraints during the rendezvous using the TSG starting from 1,000 different initial Deputy states (green dots): (a) the LoS cone angle constraint h_1 ; (b) thrust constraint h_2 ; (c) the approach velocity constraint h_3 . (d) Time history of the relative Deputy spacecraft position to the Chief spacecraft.

Figure 8a illustrates how the time shift parameter changes as a function of time. At the beginning of the simulation, we start with the initial admissible time shift parameter, $\tau_{1\mathrm{ead},0}$, and the time shift parameter, $\tau_{1\mathrm{ead}}$, is updated to the smallest admissible value by the TSG at every update step. The time shift parameter then keeps reducing until it reaches a small value for which the Deputy is able to approach the Chief.

Figure 9 shows the results of Monte Carlo simulations for different initial states of the Deputy spacecraft chosen at random, while satisfying constraints at the initial time, and corresponding to the perturbed deputy spacecraft position along the orbital track and perturbed velocity.

The constraints are enforced in all cases and the Deputy spacecraft converges to the Chief spacecraft.

V. CONCLUSIONS

In this paper, we considered the application of the time shift governor (TSG) to the spacecraft rendezvous mission in a near rectilinear halo orbit (NRHO). The TSG is shown to be capable of enforcing various constraints during the rendezvous mission, such as on the line of sight cone angle, the thrust, and the approach velocity. To enforce the constraints, the TSG commands a virtual target trajectory to the Deputy spacecraft controller, which is a time-shifted version of the Chief spacecraft trajectory. The time shift is gradually reduced to zero by the TSG so that the virtual target trajectory and the actual Chief spacecraft trajectory eventually coincide. Simulated maneuvers for NRHO in the Earth-moon system demonstrated the effectiveness of the TSG in handling constraints.

REFERENCES

- [1] S. Fuller, E. Lehnhardt, C. Zaid, and K. Halloran, "Gateway program status and overview," *Journal of Space Safety Engineering*, vol. 9, no. 4, pp. 625–628, 2022.
- [2] G. T. Coll, G. Webster, O. Pankiewicz, K. Schlee, T. Aranyos, B. Nufer, J. Fothergill, G. Tamasy, M. Kandula, A. Felt et al., "Satellite servicing projects division restore-1 propellant transfer subsystem progress 2020," in AIAA Propulsion and Energy 2020 Forum, 2020, p. 3795.
- [3] R. Biesbroek, S. Aziz, A. Wolahan, S. Cipolla, M. Richard-Noca, and L. Piguet, "The clearspace-1 mission: ESA and clearspace team up to remove debris," in 8th European Conference on Space Debris, 2021, pp. 1–3.
- [4] H. Pollard, Celestial Mechanics. American Mathematical Society, 1976, vol. 18.
- [5] P. Gurfil and P. K. Seidelmann, Celestial Mechanics and Astrodynamics: Theory and Practice. Springer, 2016, vol. 436.
- [6] K. C. Howell and H. J. Pernicka, "Numerical determination of lissajous trajectories in the restricted three-body problem," *Celestial Mechanics*, vol. 41, no. 1-4, pp. 107–124, 1987.
- [7] D. L. Richardson, "Halo orbit formulation for the ISEE-3 mission," *Journal of Guidance and Control*, vol. 3, no. 6, pp. 543–548, 1980.
- [8] L. Bury and J. W. McMahon, "Landing trajectories to moons from the unstable invariant manifolds of periodic libration point orbits," in AIAA Scitech 2020 Forum, 2020, p. 2181.
- [9] D. Guzzetti, E. M. Zimovan, K. C. Howell, and D. C. Davis, "Stationkeeping analysis for spacecraft in lunar near rectilinear halo orbits," in 27th AAS/AIAA Space Flight Mechanics Meeting, vol. 160. American Astronautical Society San Antonio, Texas, 2017, pp. 3199–3218.
- [10] M. Woodard, D. Folta, and D. Woodfork, "Artemis: The first mission to the lunar libration orbits," in 21st International Symposium on Space Flight Dynamics, Toulouse, France, 2009.
- [11] B. Cheetham, "Cislunar autonomous positioning system technology operations and navigation experiment (capstone)," in Accelerating Space Commerce, Exploration, and New Discovery 2021, 2021, p. 4128.
- [12] E. M. Zimovan, K. C. Howell, and D. C. Davis, "Near rectilinear halo orbits and their application in cislunar space," in 3rd IAA Conference on Dynamics and Control of Space Systems, Moscow, Russia, vol. 20, 2017, p. 40.
- [13] D. Scheeres and N. Vinh, "Dynamics and control of relative motion in an unstable orbit," in *Astrodynamics Specialist Conference*, 2000, p. 4135.
- [14] G. Bucchioni and M. Innocenti, "Rendezvous in cis-lunar space near rectilinear halo orbit: Dynamics and control issues," *Aerospace*, vol. 8, no. 3, p. 68, 2021.

- [15] A. Colagrossi and M. Lavagna, "Preliminary results on the dynamics of large and flexible space structures in halo orbits," *Acta Astronautica*, vol. 134, pp. 355–367, 2017.
- [16] A. W. Berning Jr, D. Liao-McPherson, A. Girard, and I. Kolmanovsky, "Suboptimal nonlinear model predictive control strategies for tracking near rectilinear halo orbits," *Astrodynamics Specialist Conference*, 2020.
- [17] P. Elango, S. Di Cairano, U. Kalabić, and A. Weiss, "Local eigenmotion control for near rectilinear halo orbits," in 2022 American Control Conference. IEEE, 2022, pp. 1822–1827.
- [18] T. Kim, S. Boone, and J. McMahon, "Higher-order feedback control law for low-thrust spacecraft guidance," *Astrodynamics Specialist Conference*, 2022.
- [19] J. C. Sanchez, F. Gavilan, and R. Vazquez, "Chance-constrained model predictive control for near rectilinear halo orbit spacecraft rendezvous," *Aerospace Science and Technology*, vol. 100, p. 105827, 2020.
- [20] N. Murakami, S. Ueda, T. Ikenaga, M. Maeda, T. Yamamoto, H. Ikeda et al., "Practical rendezvous scenario for transportation missions to cis-lunar station in earth-moon l2 halo orbit," in 25th International Symposium on Space Flight Dynamics. Munich, 2015
- [21] G. R. Frey, C. D. Petersen, F. A. Leve, E. Garone, I. V. Kol-manovsky, and A. R. Girard, "Time shift governor for coordinated control of two spacecraft formations," *International Federation of Automatic Control-PapersOnLine*, vol. 49, no. 18, pp. 296–301, 2016.
- [22] —, "Parameter governors for coordinated control of n-spacecraft formations," *Journal of Guidance, Control, and Dynamics*, vol. 40, no. 11, pp. 3020–3025, 2017.
- [23] V. Cichella, I. Kaminer, V. Dobrokhodov, E. Xargay, R. Choe, N. Hovakimyan, A. P. Aguiar, and A. M. Pascoal, "Cooperative path following of multiple multirotors over time-varying networks," *IEEE Transactions on Automation Science and Engi*neering, vol. 12, no. 3, pp. 945–957, 2015.
- [24] I. V. Kolmanovsky and J. Sun, "Parameter governors for discretetime nonlinear systems with pointwise-in-time state and control constraints," *Automatica*, vol. 42, no. 5, pp. 841–848, 2006.
- [25] A. Cotorruelo, D. Limon, and E. Garone, "Output admissible sets and reference governors: Saturations are not constraints!" *IEEE Transactions on Automatic Control*, vol. 65, no. 3, pp. 1192–1196, 2019
- [26] E. Gilbert and I. Kolmanovsky, "Nonlinear tracking control in the presence of state and control constraints: a generalized reference governor," *Automatica*, vol. 38, no. 12, pp. 2063–2073, 2002.